

# Effect of nuclear periphery on nucleon transfer in peripheral collisions

Martin Veselsky

Institute of Physics, Slovak Academy of Sciences,  
Dubravská cesta 9, Bratislava, Slovakia  
e-mail: fyzimarv@savba.sk

and

G.A. Souliotis

Cyclotron Institute, Texas A&M University,  
College Station, USA

## Abstract

A comparison of experimental heavy residue cross sections from the reactions  $^{86}\text{Kr}+^{64}\text{Ni}, ^{112,124}\text{Sn}$  with the model of deep-inelastic transfer (DIT) is carried out. A modified expression for nucleon transfer probabilities is used at non-overlapping projectile-target configurations, introducing a dependence on isospin asymmetry at the nuclear periphery. The experimental yields of neutron-rich nuclei close to the projectile are reproduced better and the trend deviating from the bulk isospin equilibration is explained. For the neutron-rich products further from the projectile, originating from hot quasiprojectiles, the statistical multifragmentation model reproduces the mass distributions better than the model of sequential binary decay. In the reaction with proton-rich target  $^{112}\text{Sn}$  the nucleon exchange appears to depend on

isospin asymmetry of nuclear periphery only when the surface separation is larger than 0.8 fm due to the stronger Coulomb interaction at more compact di-nuclear configuration.

## Introduction

Nucleus-nucleus collisions in the Fermi energy domain exhibit a large variety of contributing reaction mechanisms and reaction products ( see e.g. [1], [2], [3], [4] ) and offer the principal possibility to produce mid-heavy to heavy neutron-rich nuclei in very peripheral collisions. In the reactions of massive heavy ions such as  $^{86}\text{Kr}+^{124}\text{Sn}$  [5] and  $^{124}\text{Sn}+^{124}\text{Sn}$  [6], an enhancement was observed over the yields expected in cold fragmentation which is at present the method of choice to produce neutron-rich nuclei. Further enhancement of yields of n-rich nuclei was observed in the reaction  $^{86}\text{Kr}+^{64}\text{Ni}$  [2] in the very peripheral collisions, thus pointing to the possible importance of neutron and proton density profiles at the projectile and target surfaces.

In this article, we present an investigation of the reaction mechanism of the very peripheral nucleus-nucleus collisions with an emphasis on the possible role of different proton and neutron densities at the surface as a factor influencing the process of nucleon exchange. When nuclei with different neutron to proton ratio collide peripherally and nucleon exchange takes place, one observes equilibration of the N/Z-ratio. An isoscaling study was carried out on the reactions  $^{86}\text{Kr}+^{112}\text{Sn}$  and  $^{86}\text{Kr}+^{124}\text{Sn}$  at 25 A MeV [3] and a correlation of the isoscaling parameter with isospin equilibration was observed [7]. Peripheral nucleus-nucleus collisions can be described theoretically using the model of deep-inelastic transfer [8] in combination with an appropriate model of de-excitation. Very good description of experimental observables was obtained [2, 5, 6, 9] using the DIT model of Tassan-Got [10] and the de-excitation codes SMM [11] and GEMINI [12]. SMM represents the statistical model of multifragmentation ( SMM ) and GEMINI invokes the model of sequential binary decay ( SBD ). An enhancement of the yields of n-rich nuclei over the prediction of such calculations was observed in the reaction  $^{86}\text{Kr}+^{64}\text{Ni}$  at 25 A MeV [2]. The shapes of the velocity spectra suggested a process with a short timescale such as the very peripheral collisions where the details of neutron and proton density profiles at the projectile and target surfaces can play a significant role. An attempt was made in [5] to implement the density-dependent correction into the DIT model and an improvement

of agreement with experimental data from the reactions  $^{86}\text{Kr}+^{64}\text{Ni}$ ,  $^{112,124}\text{Sn}$  was observed for some regions, which however was not consistent enough to be conclusive and a need for further development of a self-consistent density-dependent DIT model or an equivalent approach was inferred.

## Model analysis of heavy residue data

### Reaction $^{86}\text{Kr}+^{64}\text{Ni}$

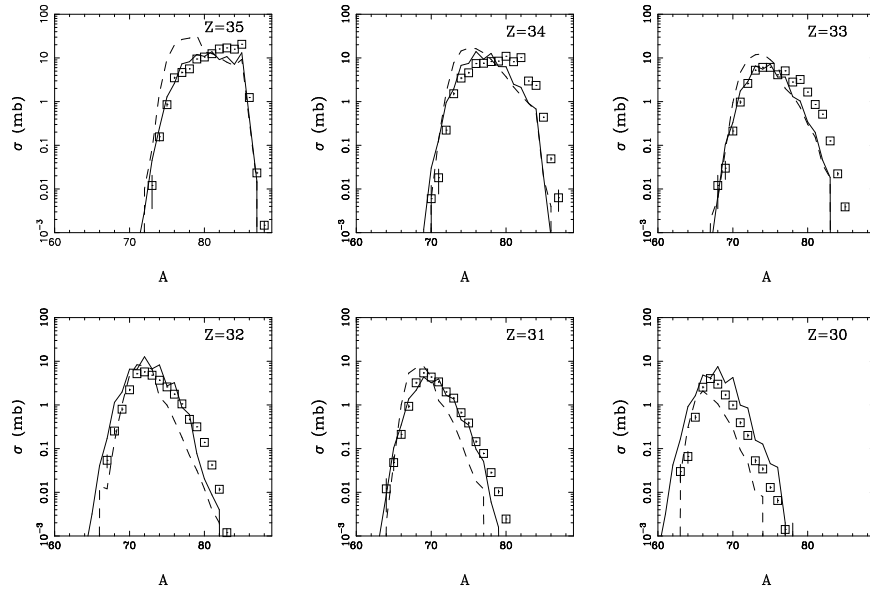


Figure 1: Experimental mass distributions ( symbols ) of elements with  $Z = 30 - 35$  observed in the reaction  $^{86}\text{Kr}+^{64}\text{Ni}$  at 25 AMeV [2] compared to the results of the standard DIT calculations combined with the de-excitation codes GEMINI and SMM ( solid and dashed line, respectively ).

In Fig. 1 we present the experimental mass distributions of elements with  $Z = 30 - 35$  observed within the separator acceptance in the reaction  $^{86}\text{Kr}+^{64}\text{Ni}$  at 25 AMeV [2] compared to the results of the standard DIT calculations [10] combined with two de-excitation codes SMM [11] ( dashed line ) and GEMINI [12] ( full line ), used for de-excitation of the quasiprojectiles emerging after the DIT stage. The simulated yields were corrected for angu-

lar acceptance of the separator positioned at  $0^\circ$  ( covering polar angles  $1.0 - 2.7^\circ$  [2] ). One observes an excess of experimental yields of neutron-rich nuclei with  $Z = 34 - 32$ , which is evident both for the SMM and the GEMINI, in the former case the effect appears to extend to lower atomic numbers. As suggested in [2], such excessive yields of neutron-rich nuclei can be caused by the effect of the neutron-rich surface of the target nucleus, which in peripheral collisions can lead to stronger flow of neutrons from the target to the projectile ( or flow of protons in the opposite direction ), thus reverting the flow toward isospin equilibration.

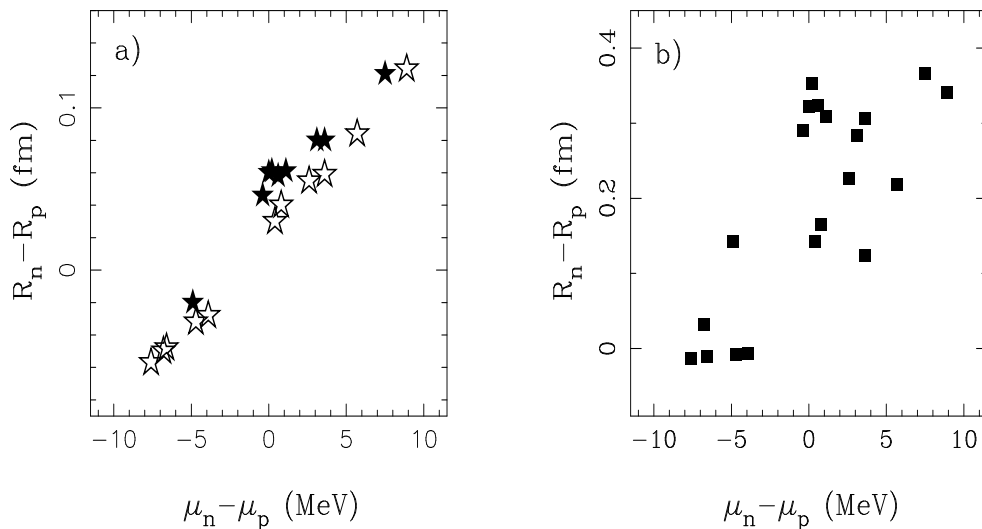


Figure 2: a) Calculated dependence of  $R_n - R_p$  on the difference of neutron and proton chemical potentials  $\mu_n - \mu_p$ , obtained using the extended Thomas-Fermi model [15]. Open and solid symbols represent the nuclei with  $A < 100$  and  $A > 100$ , respectively. b) As in a), but the values of  $R_n - R_p$  are calculated using the liquid-droplet parametrization [10, 13].

In order to understand how the properties of nuclear surface can revert the isospin flow one first needs to clarify whether and to what extent such effect of nuclear surface is implemented in the standard DIT model of Tassan-Got [10]. The model of Tassan-Got is based on various macroscopic parametrizations. For an estimate of the thickness of neutron-skin a parametrization based on liquid-droplet model of ref. [13] is used. The values of neutron-skin thickness  $t$  are then used to determine the radius of the sharp uniformly charged sphere which is used to describe the single-particle Coulomb potential [10]. Further-

more, the radius of the nuclear part of single-particle potential is additionally enhanced by 0.5 fm in order to match the typical radius of the proximity potential [14], which allows to describe the reaction dynamics properly. Thus such adjustment essentially leads to further enhancement of the thickness of neutron-rich surface. However, the relation between neutron and proton single-particle potentials and corresponding density distributions, on which the nuclear surface is usually defined, is not simple and can be, in principle, determined only in self-consistent manner. In any case, the DIT model of Tassan-Got [10] proved successful in describing the bulk N/Z-equilibration and thus explanation to the enhancement observed in Fig. 1 will be apparently related to the effects not considered in it, specifically these which will lead to modification of isospin-asymmetry at nuclear periphery. Also it is of interest to identify observables characterizing such effects.

The observable which is of particular interest is the isospin asymmetry at the nuclear periphery, specifically its deviation from the bulk isospin asymmetry of the nucleus. It can be shown that the value of this observable at the mean half-density radius  $(R_n + R_p)/2$  is determined dominantly by its linear correlation to the thickness of a neutron-rich surface  $R_n - R_p$ . An estimate of the thickness of a neutron-rich surface  $R_n - R_p$ , where  $R_n$ ,  $R_p$  are the half-density radii of neutrons and protons, can be obtained using nuclear structure calculations. A calculated dependence of  $R_n - R_p$  on the difference of neutron and proton chemical potentials  $\mu_n - \mu_p$ , obtained using the extended Thomas-Fermi code of Kolomietz et al. [15], is presented in Fig. 2, along with the liquid-droplet estimate  $R_n - R_p = 2.714((1 - 2Z/A) - 0.0016582Z/A^{1/3})/(1 + 3.45/A^{1/3})$  [10, 13]. The calculations were performed for the  $\beta$ -stable nuclei with masses  $A = 16 - 238$  (representing typical target nuclei) with the neutron-rich isotopes  $^{94}\text{Kr}$ ,  $^{132}\text{Sn}$  being added in order to extend the N/Z-range. For the extended Thomas-Fermi calculation, one observes a linear correlation for both subsets of nuclei, for heavier nuclei (solid symbols) the values of  $R_n - R_p$  appear to be somewhat larger than for lighter nuclei (open symbols), thus implying a thicker neutron-rich surface for heavier  $\beta$ -stable nuclei. The values obtained using the liquid-droplet parametrization (squares) follow similar trend, however the absolute values are significantly larger than in extended Thomas-Fermi calculation. The spread of the values is caused by the use of  $\mu_n - \mu_p$  from the previous plot, which do not follow the trend of isospin asymmetry so strictly as it is assumed in the liquid-drop model, where both  $R_n - R_p$  and  $\mu_n - \mu_p$  follow the isospin asymmetry linearly. The global correlation of  $R_n - R_p$  with

$\mu_n - \mu_p$  suggests the possibility to relate the effect of isospin asymmetry at the surface to the difference of chemical potentials. However, it should be noted that the values of  $\mu_n - \mu_p$  calculated using the extended Thomas-Fermi model represent the "smooth" ( macroscopic ) nuclear properties and may differ from the experimental values of the difference of neutron and proton separation energies  $-(S_n - S_p)$  which is typically used as the estimate of  $\mu_n - \mu_p$  for real nuclei at ground state. On the other hand, when assuming that the correlation of  $R_n - R_p$  with  $\mu_n - \mu_p$  is preserved also for real nuclei, the experimental values of  $-(S_n - S_p)$  can be assumed as representing the values of  $R_n - R_p$  of such nuclei, with the density profiles modified due to the microscopic structure, including the effects not considered in the liquid-droplet parametrization used by DIT model of Tassan-Got such as shell structure.

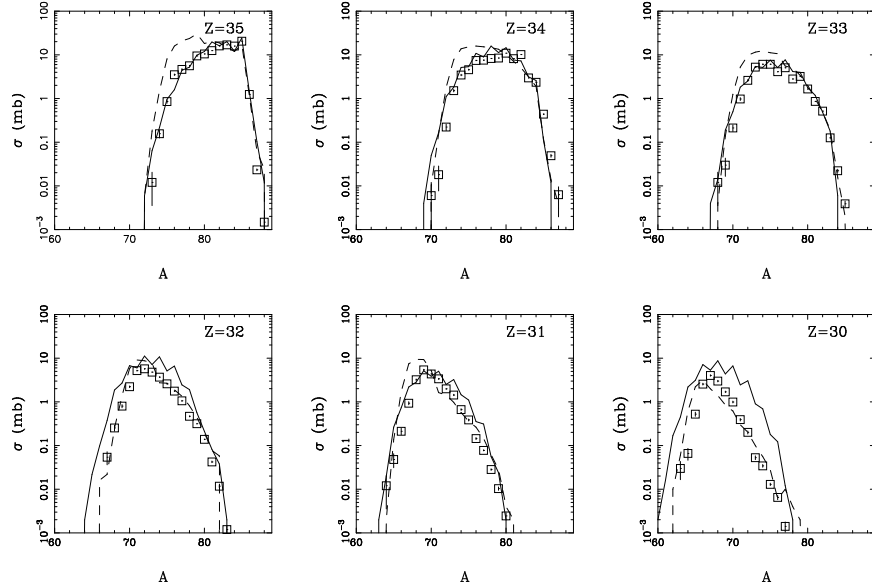


Figure 3: Experimental mass distributions ( symbols ) of elements with  $Z = 30 - 35$  observed in the reaction  $^{86}\text{Kr} + ^{64}\text{Ni}$  at 25 AMeV [2] compared to the results of the modified DIT calculations combined with the de-excitation codes GEMINI and SMM ( solid and dashed line, respectively ).

The correlation of the  $R_n - R_p$  with  $\mu_n - \mu_p$  shown in Fig. 2 suggests the possibility to implement a corresponding correction into the DIT model taking into account the effect of nuclear periphery. Based on the discussion

of Fig. 2 in the previous paragraph, in particular considering the possibility to estimate the surface properties of real nuclei using the value of  $-(S_n - S_p)$ , we made a minor modification in the DIT code of Tassan-Got [10] by scaling the transfer probabilities by the exponential factors

$$\begin{aligned}
P_n(P \rightarrow T) &\longrightarrow e^{-0.5\kappa(\delta S_{nP} - \delta S_{pP} - \delta S_{nT} + \delta S_{pT})} P_n(P \rightarrow T) \\
P_p(P \rightarrow T) &\longrightarrow e^{0.5\kappa(\delta S_{nP} - \delta S_{pP} - \delta S_{nT} + \delta S_{pT})} P_p(P \rightarrow T) \\
P_n(T \rightarrow P) &\longrightarrow e^{-0.5\kappa(\delta S_{nT} - \delta S_{pT} - \delta S_{nP} + \delta S_{pP})} P_n(T \rightarrow P) \\
P_p(T \rightarrow P) &\longrightarrow e^{0.5\kappa(\delta S_{nT} - \delta S_{pT} - \delta S_{nP} + \delta S_{pP})} P_p(T \rightarrow P)
\end{aligned} \tag{1}$$

where  $\kappa$  is a free parameter ( due to essentially a Boltzman factor structure, possibly representing an inverse statistical temperature ) and  $\delta S_{nP}$ ,  $\delta S_{pP}$ ,  $\delta S_{nT}$ ,  $\delta S_{pT}$  represent the differences of neutron and proton separation energies for the projectile and target calculated using the experimental [16] and liquid-drop [17] masses, thus expressing the effect of the microscopic structure. The smooth part is subtracted from the experimental values due to the fact that the macroscopic values of  $\mu_n - \mu_p$  follow the bulk N/Z-ratios of reaction partners and the bulk N/Z equilibration is described consistently by the DIT code of Tassan-Got. Thus, the DIT model is supplemented with phenomenological information on shell structure at the nuclear periphery which can explain the deviation of nucleon exchange from the path toward isospin equilibration, and the model framework assumes the structure commonly used e.g. to describe the ground state properties of nuclei and fission [18], where the liquid-drop model ( or extended Thomas-Fermi model in more recent works as for instance in ref. [19] ) is supplemented by additional term describing the effect of shell structure. In the present case, such a term is phenomenologically related to shell corrections in neutron and proton separation energies  $\delta S_{nP}$ ,  $\delta S_{pP}$ ,  $\delta S_{nT}$ ,  $\delta S_{pT}$ , which are based on experimental information and thus their use can result in enhanced predictive power. The modified DIT calculation was used only for non-overlapping projectile-target configurations, consistent with the assumption that it represents an effect of nuclear periphery. A cut-off was set at zero half-density surface separation ( representing touching half-density surfaces ) below which a standard DIT calculation, following the path toward isospin equilibration, was used.

In Fig. 3 we present the experimental mass distributions of elements with  $Z = 30 - 35$  observed within the separator acceptance in the reaction

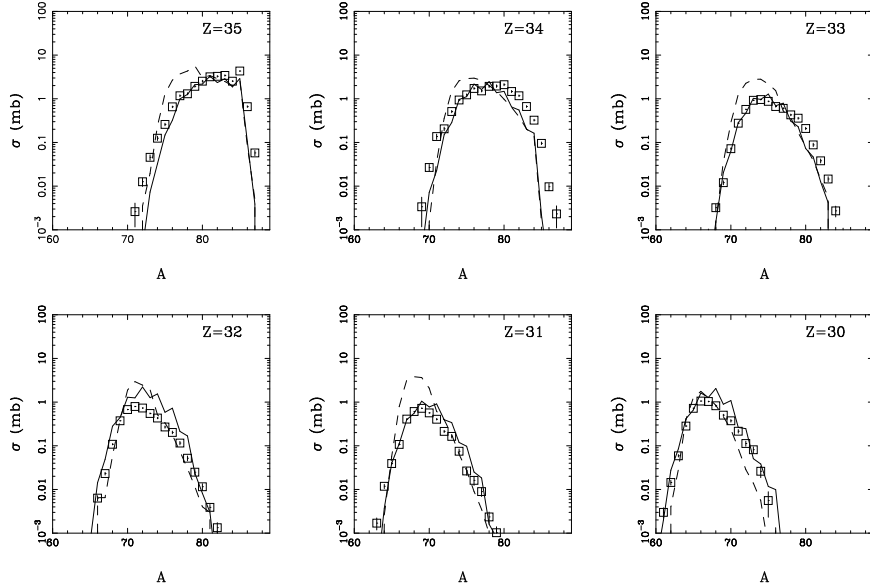


Figure 4: Experimental mass distributions ( symbols ) of elements with  $Z = 30 - 35$  observed in the reaction  $^{86}\text{Kr}+^{124}\text{Sn}$  at 25 AMeV [5] compared to the results of the standard DIT calculations with GEMINI ( full line ) and SMM ( dashed line ).

$^{86}\text{Kr}+^{64}\text{Ni}$  at 25 AMeV [2] compared to the results of the modified DIT calculations, again combined with the two de-excitation codes GEMINI [12] ( full line ) and SMM [11] ( dashed line ). The simulated yields were filtered for angular acceptance as in the case of Fig. 1. Several calculations were performed with different values of  $\kappa$  and the value of  $\kappa = 0.53$ , used in the modified DIT calculations presented in Fig. 3, was obtained as an optimum value best reproducing the experimental mass distributions. One can observe that the modification of the DIT code allows to dramatically enhance the agreement with the experimental yields of neutron-rich nuclei with  $Z = 35 - 32$  when using both de-excitation codes. The GEMINI calculation results in the nearly symmetric mass distributions which appear to overestimate the widths of mass distributions of lighter elements. The SMM calculation appears to reproduce well the yields of neutron-rich nuclei also for lighter elements, on the other hand the yields of  $\beta$ -stable isotopes appear to be overestimated. Such differences of GEMINI and SMM calculations are in good agreement with the results of the work [4] where the SMM calculations lead to better reproduction of yields originating from the hot quasiprojec-



tiles, while for the colder quasiprojectiles with excitation energies 1-2 AMeV GEMINI performed better due to the implementation of sequential binary decay which is missing in the simulation of secondary emission from the hot fragments in SMM.

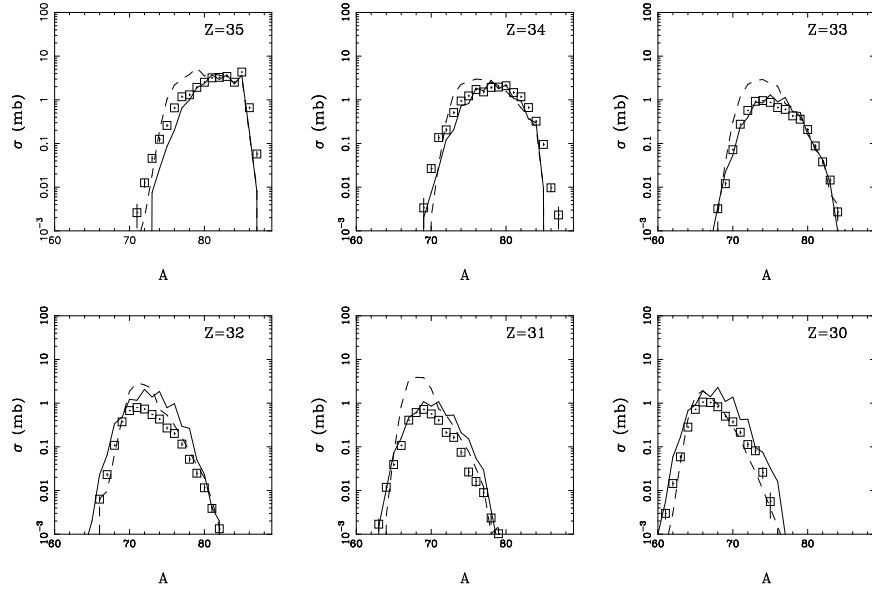


Figure 5: Experimental mass distributions ( symbols ) of elements with  $Z = 30 - 35$  observed in the reaction  $^{86}\text{Kr}+^{124}\text{Sn}$  at 25 AMeV [5] compared to the results of the modified DIT calculations with GEMINI ( full line ) and SMM ( dashed line ).

## Reactions $^{86}\text{Kr}+^{112,124}\text{Sn}$

In order to further examine the modification of the DIT code, the results of simulations were compared to data from other reactions. Figs. 4, 5 show the experimental mass distributions of elements with  $Z = 30 - 35$  observed within the separator acceptance in the reaction  $^{86}\text{Kr}+^{124}\text{Sn}$  at 25 AMeV [5] again compared to the results of the standard ( Fig. 4 ) and modified ( Fig. 5 ) DIT calculations combined with the GEMINI ( full line ) and SMM ( dashed line ). The simulated yields were filtered for angular acceptance of the separator positioned at  $4^\circ$  ( covering polar angles  $2.7 - 5.4^\circ$  [5] ) with appropriate azimuthal corrections. One can see that in this case, the overall agreement

with the experimental data is improved in the modified DIT calculation ( using  $\kappa = 0.53$  as in the previous case ) when comparing to the standard one. As in the previous case, the modified DIT calculation with SMM appears to reproduce the shapes of mass distributions more consistently ( except the overestimation of the yields of  $\beta$ -stable nuclei ), while the GEMINI code appears to lead to more symmetric mass distributions with overestimated width at lower atomic numbers.

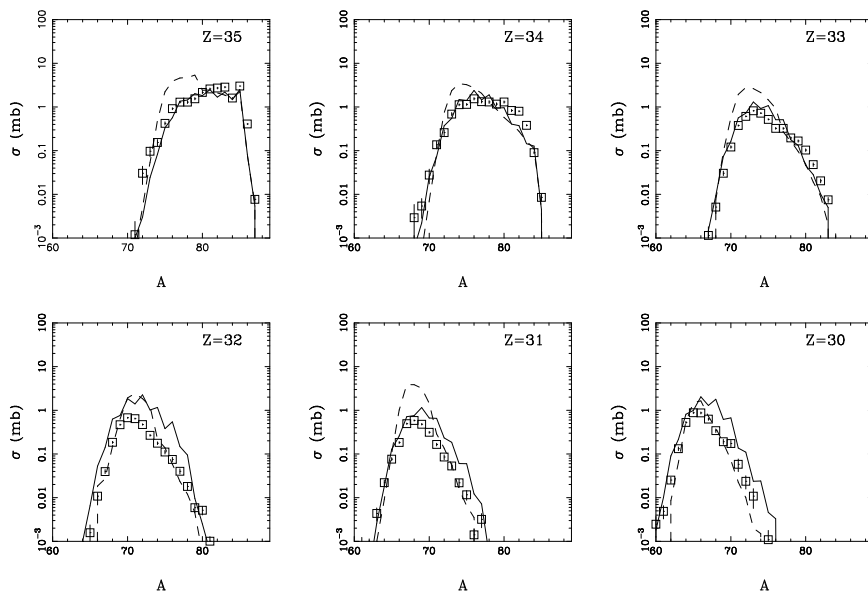


Figure 6: Experimental mass distributions ( symbols ) of elements with  $Z = 30 - 35$  observed in the reaction  $^{86}\text{Kr}+^{112}\text{Sn}$  at 25 AMeV [5] compared to the results of the standard DIT calculations with GEMINI ( full line ) and SMM ( dashed line ).

Figs. 6, 7 present the experimental mass distributions of elements with  $Z = 30 - 35$  observed within the separator acceptance in the reaction  $^{86}\text{Kr}+^{112}\text{Sn}$  at 25 AMeV [5], again compared to the results of the simulations, the standard ( Fig. 6 ) and modified ( Fig. 7 ) DIT calculations combined with the GEMINI ( full line ) and SMM ( dashed line ). The simulated yields were filtered for angular acceptance of the separator positioned at  $4^\circ$  ( as in the case of reaction  $^{86}\text{Kr}+^{124}\text{Sn}$  ). In this case the modified DIT calculation ( using the value  $\kappa = 0.53$  successful in previous cases ) combined with GEMINI leads to improvement for  $Z = 35 - 34$ , consistent with previous cases. However, both the modified and, to a lesser extent, the standard DIT calculation combined

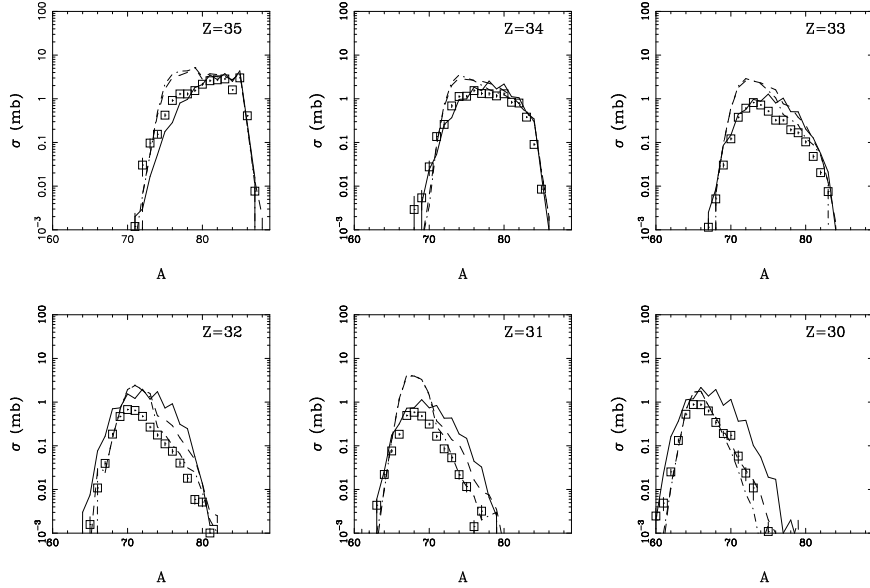


Figure 7: Experimental mass distributions ( symbols ) of elements with  $Z = 30 - 35$  observed in the reaction  $^{86}\text{Kr} + ^{112}\text{Sn}$  at 25 AMeV [5] compared to the results of the modified DIT calculations with GEMINI ( full line ) and SMM ( dashed line ). Dash-dotted line represents the modified DIT with a cutoff shifted to 0.8 fm combined with SMM.

with GEMINI appear to overestimate the yields of neutron-rich nuclei with  $Z = 33 - 30$  due to shifted centroids and overestimation of both maximum value and width. The modified DIT calculation combined with SMM appears to reproduce the shapes of mass distribution consistent to previous cases, well at the neutron-rich side ( specifically for the  $Z = 35 - 34$  ), while overestimating the yields of  $\beta$ -stable nuclei. For  $Z = 33 - 31$  the overall elemental yields appear to be overestimated ( even when subtracting the excess yields of  $\beta$ -stable nuclei ) and the standard DIT calculation combined with SMM reproduces these yields better. Such a situation in the case of the reaction  $^{86}\text{Kr} + ^{112}\text{Sn}$  may signal that an increase of proton transfer probability into such a massive proton-rich target according to Eqn. (1) may be reverted at smaller separation distances by the effect of increasingly repulsive Coulomb interaction. The dash-dotted line in Fig. 7 represents a modified DIT calculation (  $\kappa = 0.53$  ) where the cut-off is shifted to minimal separation of half-density surfaces equal to 0.8 fm, again combined with SMM. Such a cal-

ulation reproduces the experimental mass distributions much better, thus suggesting that for the proton-rich target  $^{112}\text{Sn}$ , the proton transfer barrier assumes its sensitivity to isospin asymmetry of nuclear periphery 0.8 fm outwards when compared to neutron-rich targets, due to the effect of stronger Coulomb repulsion at more compact di-nuclear configurations than predicted by the approximation used.

## Conclusions

In summary, the DIT model of Tassan-Got [10] is supplemented with a phenomenological correction introducing the effect of shell structure on nuclear periphery. A consistent agreement with experimental data is achieved in the reactions of a 25 AMeV  $^{86}\text{Kr}$  beam with three different target nuclei, specifically allowing to describe the deviation of the nucleon exchange from the path toward isospin equilibration. The value of parameter  $\kappa$  appears to be system-independent, consistent with the system-independent correlation of neutron skin thickness with difference of neutron and proton chemical potentials. The success of the modified DIT calculation can be explained as a correction reflecting the modification of neutron and proton transfer probabilities, most probably of the transfer barriers, in peripheral collisions due to the effect of shell structure on isospin asymmetry at nuclear periphery. Such an effect is of interest for better prediction of the production rates of exotic nuclei with a wide range of N/Z-ratios at the new generation of rare isotope beam facilities. Discrepancies observed for the most proton-rich target nucleus  $^{112}\text{Sn}$  signal a loss of sensitivity of the transfer barriers toward isospin asymmetry at the nuclear periphery due to increased Coulomb repulsion at non-overlapping di-nuclear configurations with surface separation below 0.8 fm. The de-excitation code GEMINI appears to systematically lead to overly symmetric mass distributions with increasingly overestimated widths toward the lighter elements. The SMM appears to reproduce the experimental shapes better ( except for excess yields of  $\beta$ -stable isotopes ). In particular the trends of the yields of neutron-rich nuclei are reproduced consistently.

This work was supported through grant of Slovak Scientific Grant Agency VEGA-2/5098/25 and by the Department of Energy through grant No. DE-FG03-93ER40773.

## References

- [1] M. Veselsky, Nucl. Phys. A 705 (2002) 193.
- [2] G.A. Souliotis et al., Phys. Lett. B 543 (2002) 163.
- [3] G.A. Souliotis et al., Phys. Rev. C 68 (2003) 24605.
- [4] M. Veselsky et al., Nucl. Phys. A 724 (2003) 431.
- [5] G.A. Souliotis et al., Phys. Rev. Lett. 91 (2003) 022701.
- [6] G.A. Souliotis et al., Nucl. Instr. Meth. B 204 (2003) 166.
- [7] G.A. Souliotis et al., Phys. Lett. B 588 (2004) 35.
- [8] J. Randrup, Nucl. Phys. A 383 (1982) 468.
- [9] M. Veselsky et al., Phys. Rev. C 62 (2000) 064613.
- [10] L. Tassan-Got, PhD Thesis, 1988, Orsay, France, IPNO-T-89-02, 1989;  
L. Tassan-Got, C. Stéfan, Nucl. Phys. A 524 (1991) 121.
- [11] J.P. Bondorf et al., Phys. Rep. 257 (1995) 133.
- [12] R. Charity et al., Nucl. Phys. A 483 (1988) 391.
- [13] W.D. Myers and W.J. Swiatecki, Nucl. Phys. A 366 (1980) 267.
- [14] J. Randrup, Nucl. Phys. A 307 (1978) 319.
- [15] V.M. Kolomietz et al., Phys. Rev. C 64 (2001) 024315.
- [16] G. Audi and A.H. Wapstra, Nucl. Phys. A 565 (1993) 1.
- [17] W.D. Myers and W.J. Swiatecki, Nucl. Phys. A 81 (1966) 1.
- [18] V.M. Strutinsky, Nucl. Phys. A 95 (1967) 420.
- [19] Y. Aboussir et al., Atomic Data and Nuclear Data Tables 61 (1995) 127.